

# A Compact Sierpinski Gasket Fractal Antenna for S, C, X, and Ku Band Applications

Ezhumalai Aravindraj<sup>1,2,\*</sup>, Ganesan Nagarajan<sup>2</sup>, and Palaniappan Ramanathan<sup>1</sup>

<sup>1</sup>Department of Electronics & Communication Engineering, Madanapalle Institute of Technology & Science, Andhra Pradesh, India

<sup>2</sup>Department of Electronics and Communication Engineering, Puducherry Technological University, Puducherry, India

**ABSTRACT:** A Sierpinski Gasket Fractal Structure embedded in an Octagonal Microstrip Printed Monopole Antenna is proposed. The prototype is mathematically developed in a miniaturized cross-sectional area with ultra-wide resonance. A fractal design resembling a third-order Sierpinski gasket is applied to the octagonal radiator in a mutually proportional manner, increases the radiation across the entire surface area by extending the effective length of the dielectric. The driven radiator exhibits Fractional Bandwidth (FBW) of 156% spanning at 2.65 GHz–21.6 GHz, along with a peak gain 6.23 dB. The fabricated prototype demonstrates excellent agreement during testing and measurement using a microwave analyzer and an anechoic chamber, respectively. The proposed antenna covers resonance for applications at the S, C, X, and Ku bands. Also, it completely envelopes the Ultra-Wideband (UWB) and Sub-6 GHz 5G spectrum.

## 1. INTRODUCTION

The need to expand the scope of microwave frequency coverage in antenna development has become increasingly essential in our daily lives. To fulfill the demands for progress in radio communication, one can utilize a single-component radiator with the ability to cover a wider spectrum of microwave frequencies [1]. In the context of mobile communication and various contemporary environments, it is essential to give significant consideration to both the size and profile of the antenna. Traditional antennas may not adequately address this particular need [2]. The effective radiators are preferred for their ability to seamless orientation with various transceiver models and provide protection against multipath interference. As a result, printed monopole antennas are utilized in specific scenarios where there is a requirement for size reduction and dynamic use of a broader range of frequencies [3]. Elevating conventional planar antennas for enhanced antenna design involves incorporating a fractal structure into the radiating element. This configuration reduces the antenna's size and enables it to function effectively across a wider frequency range, spanning from lower to higher frequencies [4]. Fractal frameworks are self-similar formations which manifest progressive fractional configurations as identical as former levels in Euclidean space [5]. Incorporating fractal patterns into printed monopole antennas leads to a notable reduction in antenna size, an extension of the effective length of the substrate, and an improvement in the propagation of EM radiation across the surface area [6, 7]. Such effects enable the formation of future generation electronic communicators and mobile phones [8, 9].

Among the conventional methods used to generate fractals, the Iterated Function System (IFS) is specifically utilized to achieve precise self-similar structures at specific vertices. The

\* Corresponding author: Ezhumalai Aravindraj (aravindraj1794@gmail.com).

antenna's resonance is adjusted and customized by choosing an appropriate fractal design [10]. The proposed design incorporates a Sierpinski gasket pattern into an octagonal-shaped printed monopole, leading to a smaller cross-sectional area for the radiator while achieving a wide resonance with increased gain [11]. In the proposed design, an electric field is channeled into the printed monopole through the utilization of a partial ground, and a lumped port is utilized to enable the transfer of electromagnetic fields between the radiator and the ground [12]. Therefore, the proposed design employs an FR-4 circuit board substrate as the dielectric material, which possesses distinctive characteristics, including a dielectric constant ( $\epsilon_r$ ) of 4.4 and a loss tangent ( $\delta$ ) of 0.02 [13].

## 2. ANTENNA DESIGN METHODOLOGIES

### 2.1. Antenna Configuration

The antenna configuration includes an octagonal radiator mounted on an FR-4 substrate, fed via a microstrip line, and features a 3<sup>rd</sup> order Sierpinski gasket fractal pattern etched at the center of the octagonal radiator. The design methodology encompasses the antenna's setup, integration of the fractal into the radiator, and the underlying operational principles of a generic antenna layout [14]. The standard representation indicating the dimensions of the radiator width and length is designated as  $W_r$  and  $L_r$ .

$$W_r = \frac{c}{2f_r \sqrt{\frac{(\epsilon_r + 1)}{2}}} \quad (1)$$

$$L_r = \left[ \frac{C}{2f_r \sqrt{\epsilon_{eff}}} \right] - 2 \left[ \frac{0.412h (\epsilon_{eff} + 0.3) \left( \frac{W_p}{t} + 0.264 \right)}{(\epsilon_{eff} - 0.258) \left( \frac{W_p}{t} + 0.8 \right)} \right] \quad (2)$$

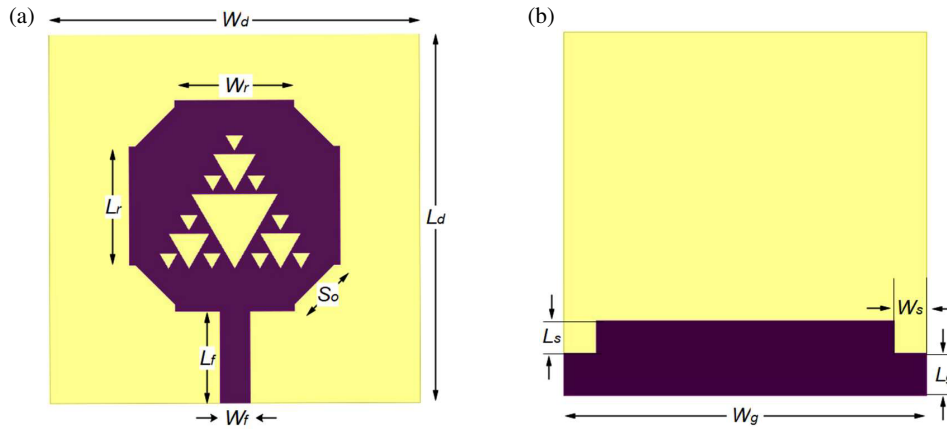


FIGURE 1. Drawings of octagonal printed monopole antenna. (a) Front view. (b) Rear view.

$$\epsilon_{eff} = \frac{\epsilon_r + 1}{2} + \frac{\epsilon_r - 1}{2} \left[ 1 + 12 \frac{t}{W} \right]^{-1/2} \quad (3)$$

Dielectric medium's length and width are represented as ( $W_d$  &  $L_d$ ), scales of radiator ( $W_r$  &  $L_r$ ) and feed line ( $W_f$  &  $L_f$ ), which are calculated using various expressions as follows:

$$W_d = 6t + W_r; \quad (4a)$$

$$L_d = 6t + L_r \quad (4b)$$

The resonant frequency ( $f_r = 3.3$  GHz), thickness of substrate ( $t = 1.6$  mm), dielectric constant of FR4 ( $\epsilon_r = 4.4$ ), and velocity of light ( $C = 3 \times 10^8$  m/s) are some of the essential parameters for the calculations. In designing a conventional radiator, the factors that impact the measurement of the associated ground and substrate are the radiator width and length [15]. As shown in Table 1, the antenna occupies a volume of  $28 \times 28 \times 1.6$  mm<sup>3</sup> and is activated through a lumped port, while it is enclosed by an open radiation boundary. Also, Figures 1(a) and (b) denote the specifications of proposed antenna in front and rear views, respectively.

$$Z_o = \frac{60 \ln \left[ \frac{S_1 t}{w_f} + \sqrt{1 + \left( \frac{2t}{w_f} \right)^2} \right]}{\sqrt{\epsilon_{eff}}} \quad (5)$$

$$S = 6 + (2\pi - 6) e^{-(30.666h/w_f)^{0.7528}} \quad (6)$$

Here,  $Z_o$  represents the characteristics impedance for the antenna while using microstrip feeding, and  $S_1$  is the supporting expressions for  $Z_o$  which in turn utilizes the width of the feed ( $W_f$ ) [16]. The proposed antenna offers approximately calculated value of  $50 \Omega$  impedance between co-axial transmission line and radiating element. Based on the specifications outlined in Table 1, the octagonal printed monopole antenna was designed using ANSYS Electronic Desktop.

## 2.2. Implementation of Sierpinski Gasket Fractal

The Sierpinski gasket geometry commences with an equilateral triangle as its base shape. Initially, the first order equilateral triangle is subdivided into three equal parts on each side, yielding

TABLE 1. Parameters and dimensions of octagonal printed monopole antenna.

Sections of Antenna	Parameters	Dimensions
Dielectric Medium	Length ( $L_d$ )	28 mm
	Width ( $W_d$ )	28 mm
	Thickness ( $t$ )	1.6 mm
Radiator	Length ( $L_r$ )	9 mm
	Width ( $W_r$ )	9 mm
	Side Notch ( $S_o$ )	3.5 mm
Ground	Length ( $L_g$ )	5.8 mm
	Width ( $W_g$ )	28 mm
Feed Line	Length ( $W_f$ )	5.8 mm
	Width ( $W_f$ )	2.3 mm
Slot	Width ( $W_s$ )	2.5 mm
	Length ( $L_s$ )	2.5 mm

new lengths that are arranged to form an additional triangle as a branch. To calculate the finite points and their positions within the vertices, the relative values of first order affine transformation matrices are utilized [18]. Figure 2 illustrates Sierpinski gasket Fractal patterns with three progressively higher levels of iterations.

Sierpinski gasket fractals are precise self-replicating structures created through the Iterated Function System (IFS) technique in combination with a generic algorithm. This approach involves representing fractal patterns within a finite set of complete metric spaces by utilizing an affine transformation matrix denoted as  $v(x, y)$ .

$$v(x, y) = \begin{bmatrix} p & q \\ r & s \end{bmatrix} \begin{bmatrix} x \\ y \end{bmatrix} + \begin{bmatrix} a \\ b \end{bmatrix} \quad (7)$$

$$v(x, y) = (px + qy + a, rx + sy + b) \quad (8)$$

When the escalating level of the contraction factor is considered, the fractal geometry is defined by a series of intricate linear matrices represented as the Hutchinson operator ( $V$ ). This

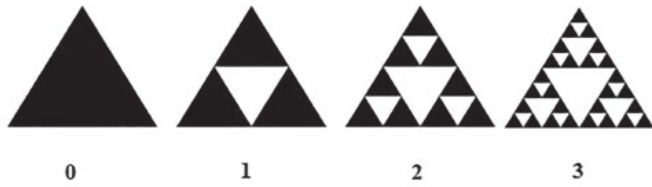


FIGURE 2. Increasing levels of Sierpinski gasket fractal pattern.

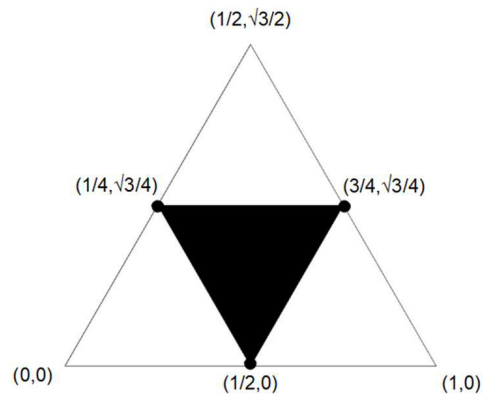


FIGURE 3. Construction of 1<sup>st</sup> order Sierpinski gasket fractal pattern in the vertices.

operator governs the vertices at each iteration level [15].

$$V(A) = \bigcup_{n=1}^3 v_n(x, y) \quad (9)$$

Hausdorff-Besicovitch formula is employed to determine the placement of a fractal structure within the Euclidean dimension ( $D$ ). It achieves this by diminishing its small-scale effect through the reversal of the scaling factor ( $S$ ) and maintaining equilibrium in the count of self-similar branches ( $N$ ) [16]. Therefore, the Hausdorff-Besicovitch formula can be represented as follows:

$$N = S^D \quad (10)$$

$$\log_{10}(N) = D \log_{10}(S) \quad (11)$$

The affine transformation matrices for the proposed design of the Sierpinski gasket fractal are represented below:

$$v(x, y) = \begin{bmatrix} a \cos \theta & c \sin \theta \\ b \sin \theta & d \cos \theta \end{bmatrix} \begin{bmatrix} x \\ y \end{bmatrix} + \begin{bmatrix} x_0 \\ y_0 \end{bmatrix} \quad (12)$$

$$v_1(x, y) = \begin{bmatrix} \frac{1}{2} & 0 \\ 0 & \frac{1}{2} \end{bmatrix} \begin{bmatrix} x \\ y \end{bmatrix} + \begin{bmatrix} \frac{1}{2} \\ 0 \end{bmatrix} \quad (13)$$

$$v_2(x, y) = \begin{bmatrix} \frac{1}{2} & 0 \\ 0 & \frac{1}{2} \end{bmatrix} \begin{bmatrix} x \\ y \end{bmatrix} + \begin{bmatrix} \frac{1}{4} \\ \frac{\sqrt{3}}{4} \end{bmatrix} \quad (14)$$

$$v_3(x, y) = \begin{bmatrix} \frac{1}{2} & 0 \\ 0 & \frac{1}{2} \end{bmatrix} \begin{bmatrix} x \\ y \end{bmatrix} + \begin{bmatrix} \frac{3}{4} \\ \frac{\sqrt{3}}{4} \end{bmatrix} \quad (15)$$

As shown in Figure 3, the Sierpinski gasket fractal pattern emerges when a solid triangle is partitioned into four smaller equilateral triangles by employing the midpoints of the three sides of the initial triangle as the vertices for the new triangles. With reference to the three outer triangles, the middle boundary will be removed. The 1<sup>st</sup> order can be derived by scaling three replicas of 0<sup>th</sup> order, each by a factor of 1/2, and subsequently translating two of the smaller triangles to create the intended configuration. Hence, the result of intersecting all sets within this sequence essentially represents the collection of points that persist after the repetition of this fractal construction an infinite number of times.

### 2.3. Operating Principle

The final design comprises an octagonal printed monopole with an embedded Sierpinski fractal pattern and a partial ground. This configuration is fed using a microstrip feeding technique. The proposed design utilizes a fractal pattern within an octagonal printed monopole radiator, along with two edge slits in the partial ground, to enhance bandwidth. The incorporation of cutting truncation and cut edges in the Sierpinski triangles with octagonal radiator induces more discontinuity in directed radiation from the antenna. This proposed design will also progressively eliminate reflections and improve bandwidth. The edge truncated fractal structure in the radiator of this antenna design facilitates efficient reflection and current distribution at the surface boundary printed monopole.

As detailed in last section, the Sierpinski gasket pattern is constructed with a third-order iterative level using the Iterated Function System (IFS) technique and is incorporated into the octagonal printed monopole to facilitate size reduction and enhance the antenna's radiation characteristics. The iteration level is limited at the 3<sup>rd</sup> order to prevent discrepancies in antenna measurements during the fabrication process particularly due to the utilization of the prototype at a scale of a few millimeters. The simulated antenna is designed and analyzed using High-Frequency Structure Simulator (HFSS) Tool, and the designed antenna is fabricated using Milling method. The overall dimensions of the proposed Sierpinski gasket fractal antenna are  $28 \times 28 \times 1.6 \text{ mm}^2$ . Figures 4(a) and (b) show the front and rear views of the physical antenna prototype manufactured through milling.

## 3. RESULTS AND DISCUSSION

### 3.1. Bandwidth

When examining the  $S_{11}$  parameter of the designed and manufactured antennas, it becomes evident that both antennas provide a bandwidth about 18.6 GHz, i.e., Fractional Bandwidth (FBW) of 160%, and exhibit a significant correlation.

From the return loss plot depicted in Figure 5, it is determined that the simulated antenna with Sierpinski gasket fractal pattern operates across a wider frequency range (2.3 GHz to 20.9 GHz)

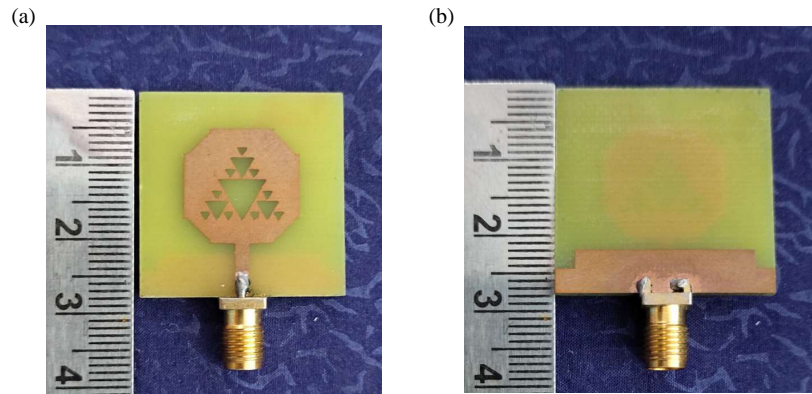


FIGURE 4. Fabricated octagonal Sierpinski gasket fractal antenna. (a) Front view. (b) Rear view.

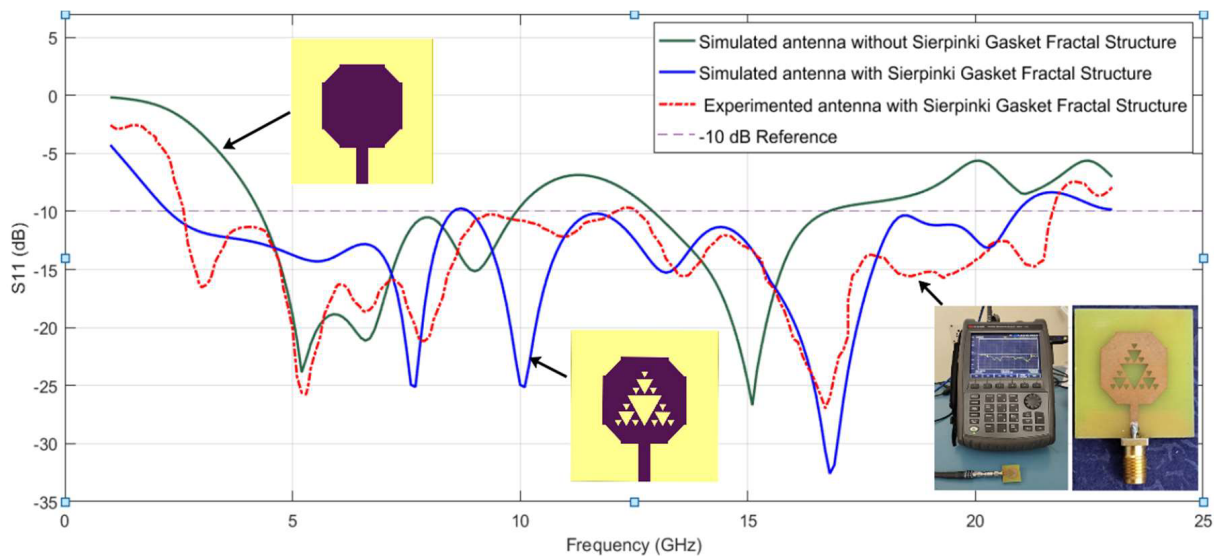


FIGURE 5. Return loss.

than the simulated antenna without Sierpinski gasket fractal structure which operates only from 4.28 GHz to 18.56 GHz, and the fabricated antenna with Sierpinski gasket fractal pattern operates over the frequency band of 2.65 GHz to 21.6 GHz. This indicates a fractional bandwidth (FBW) of 160.3% for the proposed simulated antenna with Sierpinski fractal and a 156.2% FBW for the fabricated antenna with Sierpinski fractal. Also, the bandwidth ratios obtained from the simulated and fabricated antenna are 9.08 : 1 and 8.15 : 1, respectively.

From the comparison, it is evident that the simulated and experimented antennas with Sierpinski gasket fractal pattern perform better than the conventional octagonal printed monopole antenna. Hence, both simulated and experimented antennas provide an extended bandwidth and demonstrate a valid concurrence with one another.

### 3.2. Gain

Figure 6(a) represents the gain of the simulated antenna, and Figure 6(b) depicts the orientation and 3-D view of how the ra-

diation emerges for the proposed antenna. A close examination of the three-dimensional gain pattern reveals that the antenna displays an omnidirectional radiation pattern, allowing it to radiate in all directions across a 360-degree span. At 17 GHz, the simulated antenna attains a peak gain of 6.23 dB and a peak directivity value of 6.45 dB. Due to the symmetry structure of the proposed antenna, this work focuses on the far-field results during feed excitation. Figure 6 illustrates the peak gain of the antenna in the  $y$ -direction.

### 3.3. Radiation Pattern

The radiation patterns of the proposed antenna at resonant bands (9 GHz, 11 GHz, and 18 GHz) are considered in  $xz$ -plane and  $yz$ -plane for gain total radiation measurements making  $\theta = 0^\circ$  to  $360^\circ$  and  $\phi = 0^\circ$ ,  $\phi = 90^\circ$ ;  $\phi = 0^\circ$  to  $360^\circ$  and  $\theta = 0^\circ$ ,  $\theta = 90^\circ$  are shown in Figures 7(a), 7(b), 8(a), 8(b), 9(a), and 9(b). The Left-Hand Circularly Polarized (LHCP) is depicted in Figures 7(c), 8(c), and 9(c), and Right-Hand Circularly Polarized (RHCP) is depicted in Figures 7(d), 8(d),

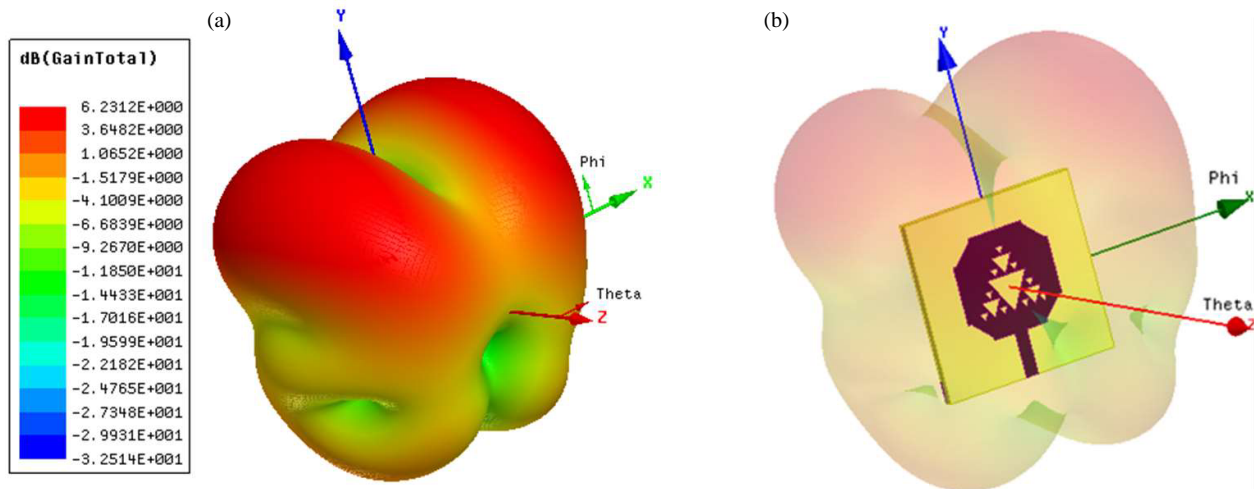


FIGURE 6. Gain.

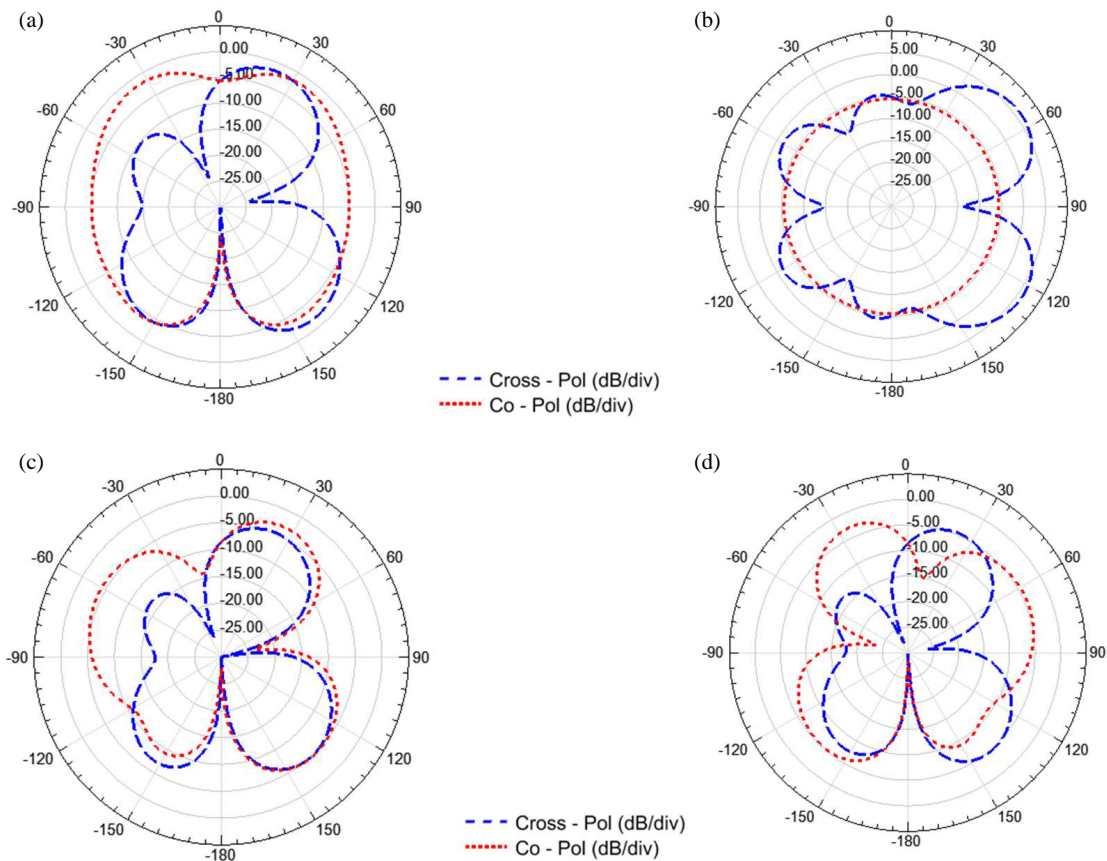


FIGURE 7. Radiation pattern (gain) at 9 GHz. (a) *E*-plane, (b) *H*-plane, (c) LCHP, (d) RCHP.

and 9(d) for 9 GHz, 11 GHz, and 18 GHz, respectively. The printed monopole is designed to achieve an improved radiation characteristic, excited through the port via *E*-plane coupling in the *xz*-direction and *H*-plane coupling in the *yz*-direction at the resonating frequencies. Here, Co-Polarization and Cross Polarization configurations are measured with respect to dB at the all-specified angles.

In the case of the fabricated antenna, gain is quantified in terms of power (dB). The antenna is positioned at the receiver station in the anechoic chamber, and received power is gauged in both the *E*-plane (antenna prototype placed vertically) and *H*-plane (antenna prototype placed horizontally), as depicted in Figures 10(a) and (b), respectively. The transmitter is a Horn antenna which is capable of transmitting 1 GHz to 20 GHz. The

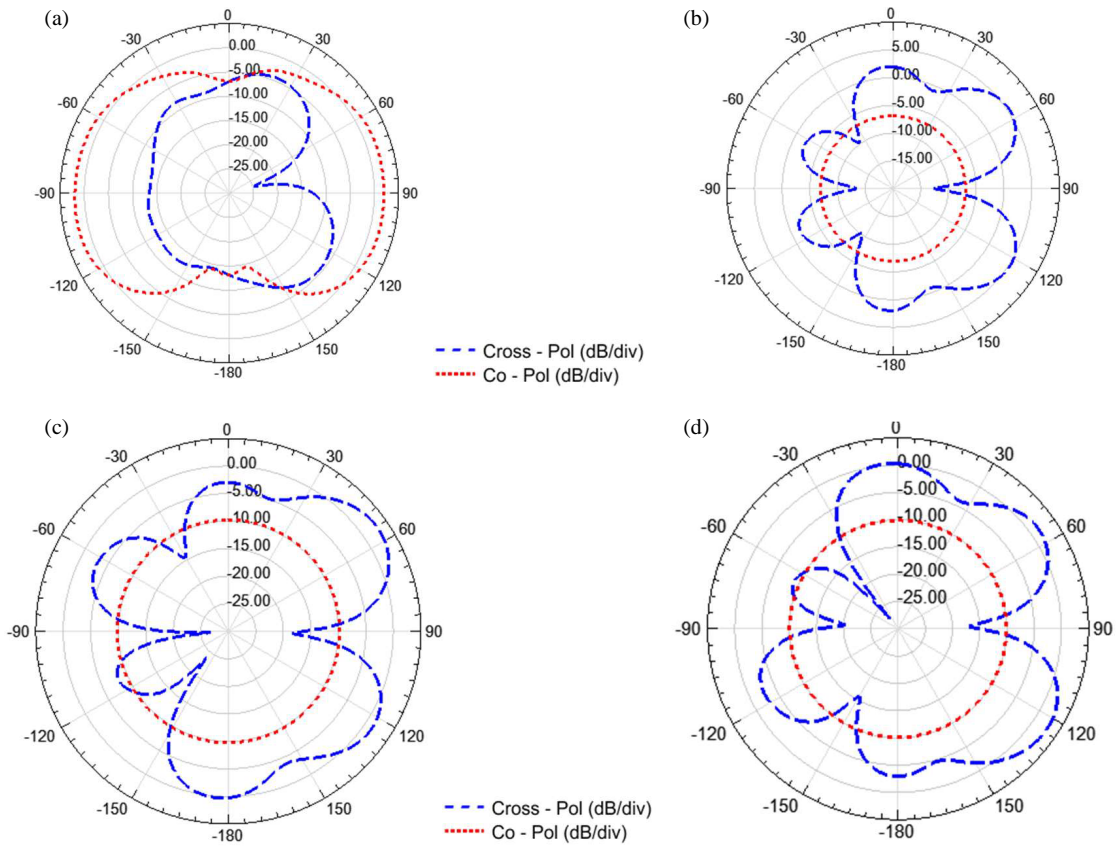


FIGURE 8. Radiation pattern (gain) at 11 GHz. (a) *E*-plane, (b) *H*-plane, (c) LCHP, (d) RCHP.

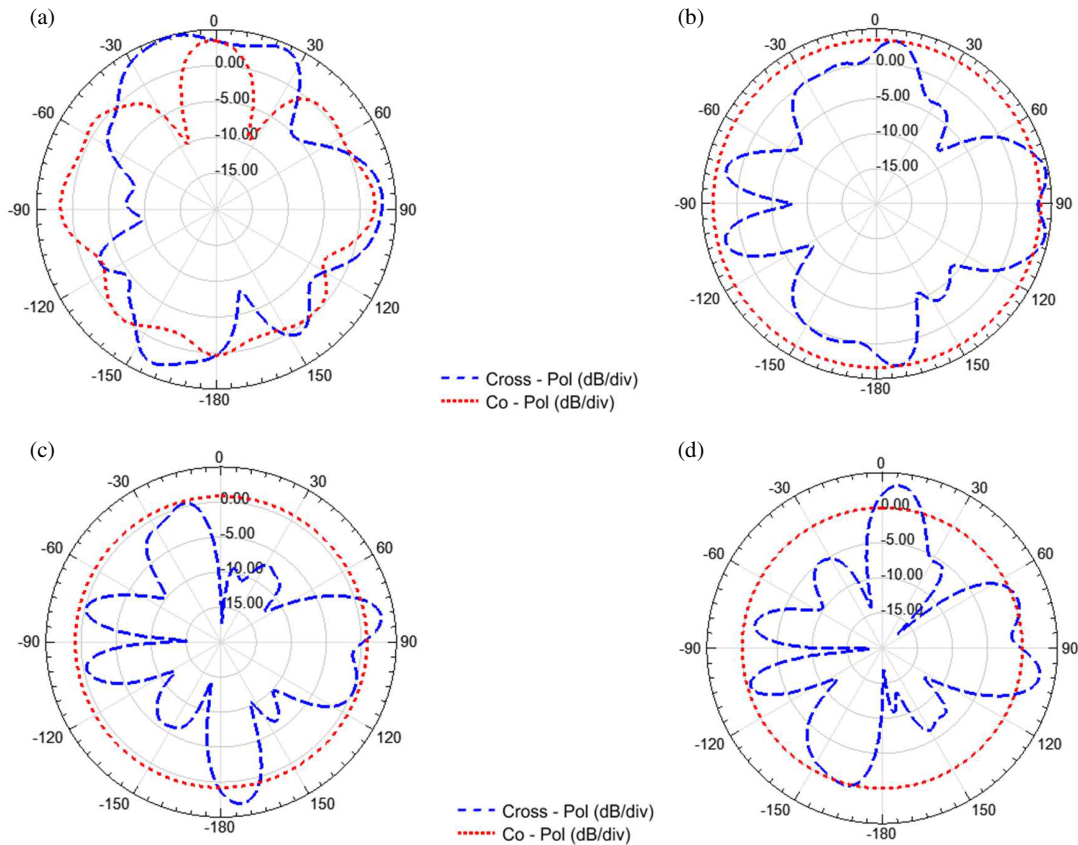


FIGURE 9. Radiation pattern (gain) at 18 GHz. Radiation pattern (gain) at 11 GHz. (a) *E*-plane, (b) *H*-plane, (c) LCHP, (d) RCHP.

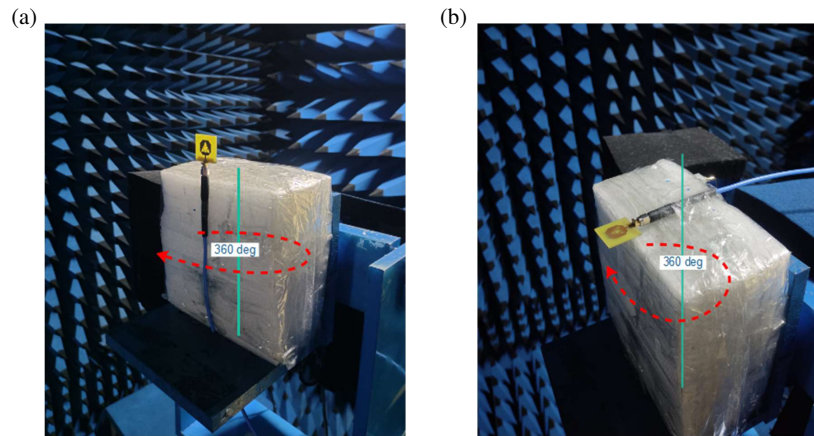


FIGURE 10. *E*-plane and *H*-plane arrangement of fabricated antenna in anechoic chamber. (a) *E*-plane, (b) *H*-plane.

TABLE 2. Comparison of proposed work with some recent existing works.

Ref./Prop. Work	Dimensions (mm <sup>3</sup> )	Frequency Range (GHz)	FBW (%)	Gain (dB)	BW Ratio
[17]	24 × 22 × 1.57	3.1–11	112.05	4	4.07 : 1
[18]	18.5 × 39 × 1.59	3.2–12	115.78	4.7	4.52 : 1
[19]	34 × 34 × 1.5	3.2/4.8	62.5	3.72	2.17 : 1
[20]	41 × 99.4 × 3.245	4.3–11.6	91.8	4.7	3.85 : 1
[21]	38 × 36 × 1.4	3–21.5	151	5	7.16 : 1
[22]	52 × 46 × 1.6	2.2–8.4	116.9	4.4	3.81 : 1
[23]	46 × 46 × 0.8	3.1–12	117	4	3.87 : 1
[24]	30 × 30 × 1.6	4.1–19.8	131	6.1	4.8 : 1
<b>Sim. Results</b>	<b>28 × 28 × 1.6</b>	<b>2.3–20.9</b>	<b>160.3</b>	<b>6.23</b>	<b>9.08 : 1</b>
<b>Expt. Results</b>	<b>28 × 28 × 1.6</b>	<b>2.65–21.6</b>	<b>156.2</b>	<b>6.15</b>	<b>8.15 : 1</b>

transmitting (Horn) antenna and receiving (Sierpinski gasket printed monopole) antenna are placed 2 meters away. The orientation transmitting antenna is set to be stable, and the receiver antenna is made to rotate along the axis from left to right at 360° which are also denoted in Figure 10. Through it, the transmitted power will be received by the Sierpinski gasket printed antenna along all 360° in *E*-plane. The delivered power ( $w$ ) is observed, and it is converted into gain (dB). Hereby, the actual antenna gain can be computed using Friis transmission equation which can be expressed as

$$G_r = P_r - P_t - G_t - 20 \log \left( \frac{c}{4\pi R f_r} \right) \text{ (dB)} \quad (16)$$

where  $R$  is the distance between the transmitting and receiving antennas;  $P_r$  is the received power;  $G_r$  is the receiver gain;  $P_t$  is the transmitted power;  $G_t$  is the transmitter gain;  $f_r$  is the radiating frequency.

In Table 2, a comparison of the proposed work (Simulated Results and Experimented Results) with recent existing studies, considering parameters such as antenna dimensions, radiated frequencies, fractional bandwidth, and antenna gain is presented. The table distinctly shows that the proposed antenna outperforms others in terms of output parameters.

## 4. CONCLUSION

In this proposed work, a Sierpinski gasket fractal embedded octagonal printed monopole antenna with a defective ground structure which can be utilized for various wireless applications is simulated and fabricated. The simulated configuration demonstrates a 6.23 dB of peak gain and an FBW of 160%, covering a range from 2.3 GHz to 20.9 GHz. Furthermore, the antenna is physically created through the milling process, and the resulting prototype provides an FBW of 156% spanning at 2.65 GHz–21.6 GHz, along with a peak gain 6.15 dB. These parameters were assessed and obtained using a microwave analyzer and an anechoic chamber, respectively. Thus, the proposed antenna envelopes an overall range of operating frequencies which are suitable for S, C, X, and Ku-band applications. Also, it completely wraps the Ultra-Wideband (UWB) and Sub-6 GHz 5G spectrum.

## REFERENCES

- [1] Visser, H. J., *Antenna Theory and Applications*, 1–13, John Wiley & Sons, 2012.
- [2] Balanis, C. A., *Antenna Theory: Analysis and Design*, 4th ed., 783–858, John Wiley & Sons, 2016.

- [3] Milligan, T. A., *Modern Antenna Design*, 2nd ed., 287–293, John Wiley & Sons, 2005.
- [4] Barnsley, M. F., *Fractals Everywhere*, 2nd ed., 171–195, Academic Press, 1993.
- [5] Aravindraj, E., K. Ayyappan, and R. Kumar, “Performance analysis of rectangular MPA using different substrate materials for WLAN application,” *ICTACT Journal on Communication Technology*, Vol. 8, No. 1, 1447–1452, 2017.
- [6] Falconer, K., *Techniques in Fractal Geometry*, 156–186, John Wiley & Sons, 1997.
- [7] Mandelbrot, B. B., *The Fractal Geometry of Nature*, 595–598, W. H. Freeman and Company, 1983.
- [8] Aravindraj, E. and K. Ayyappan, “Design of slotted H-shaped patch antenna for 2.4 GHz WLAN applications,” in *2017 International Conference on Computer Communication and Informatics (ICCCI)*, 1–5, Coimbatore, India, Jan. 2017.
- [9] Pandey, U., P. Singh, R. Singh, N. P. Gupta, S. K. Arora, and E. Nizeyimana, “Miniaturized ultrawideband microstrip antenna for IoT-based wireless body area network applications,” *Wireless Communications and Mobile Computing*, Vol. 2023, 1–19, 2023.
- [10] Ezhumalai, A., N. Ganesan, and S. Balasubramaniyan, “An extensive survey on fractal structures using iterated function system in patch antennas,” *International Journal of Communication Systems*, Vol. 34, No. 15, 1–38, 2021.
- [11] Raj, A., D. C. Dhukarya, D. K. Srivastava, and D. Mandal, “Design and analysis of square shape slot cut high gain sierpinski carpet fractal antenna for wireless applications,” *Microwave and Optical Technology Letters*, Vol. 65, No. 8, 2337–2343, 2023.
- [12] Markkandan, S., C. Malarvizhi, L. Raja, J. Kalloor, J. Karthi, and R. Atla, “Highly compact sized circular microstrip patch antenna with partial ground for biomedical applications,” *Materials Today: Proceedings*, Vol. 47, 318–320, 2021.
- [13] Nejd, I. H., S. Bri, M. Marzouk, S. Ahmad, Y. Rhazi, M. A. Lafkih, Y. A. Sheikh, A. Ghaffar, and M. Hussein, “UWB circular fractal antenna with high gain for telecommunication applications,” *Sensors*, Vol. 23, No. 8, 1–15, 2023.
- [14] Sood, M. and A. Rai, “Design of compact fractal patch antenna for X/Ku/K-band applications,” *International Journal of Communication Systems*, Vol. 36, No. 11, 1–13, 2023.
- [15] Aravindraj, E., G. Nagarajan, and R. S. Kumaran, “Design and analysis of recursive square fractal antenna for WLAN applications,” in *2020 International Conference on Emerging Trends in Information Technology and Engineering (IC-ETITE)*, 1–5, Vellore, India, Feb. 2020.
- [16] Sharma, S., C. Tripathi, and R. Rishi, “Impedance matching techniques for microstrip patch antenna,” *Indian Journal of Science and Technology*, Vol. 10, No. 28, 1–16, 2017.
- [17] Soleimani, H. and H. Orazi, “Miniaturization of UWB triangular slot antenna by the use of dual-reverse-arrow fractal,” *IET Microwaves, Antennas & Propagation*, Vol. 11, No. 4, 450–456, Mar. 2017.
- [18] Gorai, A., M. Pal, and R. Ghatak, “A Compact fractal-shaped antenna for ultrawideband and Bluetooth wireless systems with WLAN rejection functionality,” *IEEE Antennas and Wireless Propagation Letters*, Vol. 16, No. 5, 2163–2166, Mar. 2017.
- [19] Kadhim, M. A., M. F. Mosleh, and S. A. Shandal, “Wideband square Sierpinski fractal microstrip patch antenna for various wireless applications,” in *IOP Conference Series: Materials Science and Engineering*, Vol. 518, No. 4, 1–18, 2019.
- [20] Sohi, A. K. and A. Kaur, “A complementary Sierpinski gasket fractal antenna array integrated with a complementary Archimedean defected ground structure for portable 4G/5G UWB MIMO communication devices,” *Microwave and Optical Technology Letters*, Vol. 62, No. 7, 2595–2605, 2020.
- [21] Dastranj, A., F. Ranjbar, and M. Bornapour, “A new compact circular shape fractal antenna for broadband wireless communication applications,” *Progress In Electromagnetics Research C*, Vol. 93, 19–28, 2019.
- [22] Orugu, R. and N. Moses, “Triangular fractal loaded reconfigurable antenna with notch band characteristics,” *International Journal of Numerical Modelling: Electronic Networks, Devices and Fields*, Vol. 34, No. 1, e2806, 2021.
- [23] Debnath, P., A. Karmakar, A. Saha, and S. Huda, “UWB MIMO slot antenna with Minkowski fractal shaped isolators for isolation enhancement,” *Progress In Electromagnetics Research M*, Vol. 75, 69–78, 2018.
- [24] Aravindraj, E., G. Nagarajan, and R. S. Kumaran, “A monopole octagonal Sierpinski carpet antenna with defective ground structure for SWB applications,” in *Springer Lecture Notes in Electrical Engineering: Machine Learning, Deep Learning and Computational Intelligence for Wireless Communication*, Vol. 749, 267–280, 2021.